Journal of Alloys and Compounds 613 (2014) 226–231

Contents lists available at ScienceDirect

Journal of Alloys and Compounds

journal homepage: www.elsevier.com/locate/jalcom

Preparation of high performance $CaAlSiN_3:Eu^{2+}$ phosphors with the aid of BaF_2 flux

Wei-Wei Hu [a], Chao Cai [a], Qiang-Qiang Zhu [a], Xin Xu [a], Lu-Yuan Hao [a,*], Simeon Agathopoulos [b]

[a] Chinese Academy of Sciences Key Laboratory of Materials for Energy Conversion, Department of Materials Science and Engineering, University of Science and Technology of China, Hefei, Anhui 230026, People's Republic of China
[b] Materials Science and Engineering Department, University of Ioannina, GR-451 10 Ioannina, Greece

ARTICLE INFO

Article history:
Received 4 April 2014
Received in revised form 3 June 2014
Accepted 4 June 2014
Available online 12 June 2014

Keywords:
Optical materials
Solid state reactions
Optical properties
Thermal analysis
Luminescence

ABSTRACT

A strong red-emitting Eu^{2+} activated $CaAlSiN_3$ phosphor was successfully prepared by a pressureless low temperature solid-state reaction method with the aid of fluxes, namely BaF_2, CaF_2, NH_4F, and H_3BO_3. The experimental results showed that the addition of BaF_2 flux effectively reduced the temperature of formation of $CaAlSiN_3:Eu^{2+}$ by about 100 K and suppressed the volatilization of the raw materials, suggesting that BaF_2 flux modifies the mechanism of formation of $CaAlSiN_3:Eu^{2+}$. The powder of the $CaAlSiN_3:Eu^{2+}$ phosphor produced with 6 wt% BaF_2 flux had an enhanced emission intensity, which was a result of the high crystallinity, the absence of secondary phases, the narrow particle-size distribution, and the clean surfaces of the particles in the final product.

1. Introduction

A wide variety of nitride or oxynitride phosphors have been developed recently for use in white light emitting diodes [1–4]. Many silicon-nitride and -oxynitride based materials have been extensively investigated, such as $BaSi_3Al_3O_4N_5:Eu^{2+}$ [5], $MSi_2O_2N_2:Eu^{2+}$ (M = Ca, Sr, Ba) [6–9], Ca-α-SiAlON:Eu^{2+} [10,11], $LaSi_3N_5:Ce^{3+}$ (Eu^{2+}) [12,13], $M_2Si_5N_8:Eu^{2+}$ (M = Ca, Sr, Ba) [14–16], and $CaAlSiN_3:Eu^{2+}$ [17–21]. Owing to the advantages of these rare-earth doped phosphors, including strong absorption from the UV to the blue region, high quantum efficiency, and excellent thermal quenching characteristics compared to oxide and sulfide-based phosphors, they are vastly used as efficient conversion phosphors for white-LEDs.

Among nitride phosphors, red-emitting phosphors have gained increasing attention because of the broad band emission in the red-light wavelength range, which significantly enhances the color rendering index of white LEDs. So far, only nitride phosphors have been commercialized as highly efficient red-emitting phosphors for white-LEDs. Recently, $CaAlSiN_3:Eu^{2+}$ has attracted considerable interest due to its high quantum efficiency, excellent thermal properties, and chemical stability. Consequently, there are many research efforts directed towards the development of novel and promising methods of synthesizing $CaAlSiN_3$ phosphors [22–25].

Commercial $CaAlSiN_3$ phosphors are usually synthesized with a solid-state reaction at temperatures between 1600 and 1800 °C in a nitrogen atmosphere with a pressure of 0.5–1.0 MPa [25,26]. However, this method is rather complex and highly energy consuming. In the literature, there are reports which have postulated that the use of fluxes can improve the photoluminescence properties of nitride phosphors [27,28]. However, there are no works that systematically report on the effect of fluxes in the case of $CaAlSiN_3$ phosphors.

This paper presents the influence of fluxes, namely BaF_2, CaF_2, NH_4F, and H_3BO_3, incorporated in the synthesis process of $CaAlSiN_3:Eu^{2+}$ phosphors on the particle size and morphology of the produced powders and their crystalline structure and photoluminescence (PL) properties as well as the mechanism of the solid state reaction employed to synthesize these phosphors. With regard to the amount of Eu in the $Ca_{1-x}AlSiN_3:Eu_x^{2+}$ phosphors, earlier studies have shown that $CaAlSiN_3$:1.6%Eu^{2+} has the optimum quantum output [26]. Thus, in this work, we have chosen this composition (i.e. $x = 0.016$) as the reference composition.

2. Materials and experimental procedure

Fine powders of high purity Ca_3N_2, AlN (Grade F, Tokuyama Soda Co., Tokyo, Japan), Si_3N_4 (NP500 grade, Denki Kagaku Kogyo Co., Tokyo, Japan, d50 = 0.5 lm), and EuN were used. The binary nitride precursors of Ca_3N_2 and EuN were prepared

* Corresponding author. Address: Jinzhai Road 96, Hefei, Anhui, People's Republic of China. Tel.: +86 551 63600834; fax: +86 551 63601592.
E-mail address: hly@ustc.edu.cn (L.-Y. Hao).

http://dx.doi.org/10.1016/j.jallcom.2014.06.026
0925-8388/

by a gas–solid reaction. Pure calcium metal (99.5%) and europium metal (99.5%) were loaded into a BN crucible and heated to 750 °C within 360 min in a horizontal tube furnace under purely dried nitrogen and held at this temperature for 8 h. The fluxes used were also fine powders of BaF_2, CaF_2, NH_4F, and H_3BO_3 and all the fluxed were from Sinopharm Chemical Reagent Co., Ltd. (Shanghai, China). The powders, at the precise weight according to the required stoichiometry, were thoroughly mixed and ground in a glove box where oxygen and moisture contents were maintained below 1 ppm. The powder mixture was put into BN crucibles and fired at 1600 °C for 4 h under a flowing nitrogen gas atmosphere. The heating rate was 300 K/h, and after firing the samples were cooled down naturally inside the furnace. Synthesis was also carried out at 1700–1800 °C under a static N_2 gas with a pressure of 0.5 MPa.

To shed light on the mechanism of formation of $Ca_{1-x}AlSiN_3:Eu_x^{2+}$ phosphors from the raw materials with increasing temperature, small amounts of the homogenous powder mixtures (not fired) were subjected to thermal analysis. In particular, differential scanning calorimetry and thermogravimetric analyses (DSC/TG) were carried out in flowing N_2 from room temperature to 1400 °C at a heating rate of 10 K/min using a DTG-60H detector (Shimadzu, Kyoto, Japan).

Crystalline phase analysis of the produced phosphor powders was done in an X-ray diffractometer (model PW 1700, Philips Research Laboratories, Eindhoven, the Netherlands) using Cu Kα radiation at a scanning rate of 0.5 °/min. The morphology of the powders was observed by scanning electron microscopy (SEM, JSM-6390LA, JEOL, Tokyo, Japan). Their PL spectra were recorded at room temperature by a fluorescence spectrophotometer (model F-4600, Hitachi, Tokyo, Japan) with a 200 W Xe lamp as an excitation source. The emission spectrum was corrected for the spectral response of the monochromator and Hamamatsu R928P photomultiplier tube (Hamamatsu Photonics K.K., Hamamatsu, Japan) by a light diffuser and tungsten lamp (Noma Electric Corp., New York, NY; 10 V, 4 A). The excitation spectrum was also corrected for the spectral distribution of the xenon lamp intensity by measuring rhodamine-B as a reference.

3. Results and discussion

The influence of fluxes (added in an amount of 6 wt%) on the crystalline structure of $Ca_{0.984}AlSiN_3:Eu^{2+}_{0.016}$ phosphors produced after calcination at 1600 °C for 4 h is shown in the diffractograms in Fig. 1. The standard XRD pattern of $CaAlSiN_3$ in Fig. 1 was reported by Piao [17]. It is clearly seen that pure $CaAlSiN_3$ was predominantly produced in the case of both the flux-free phosphor and the phosphors with the addition of fluxes. Weak peaks of a secondary phase of AlN were also recorded. There is no evidence of peaks related to the fluxes. The addition of BaF_2 and CaF_2 fluxes resulted in a single-phase $CaAlSiN_3$ powder and the corresponding diffractograms had the strongest peaks. On the other hand, the diffractogram of the phosphor with the addition of H_3BO_3 flux had the weakest peaks of $CaAlSiN_3$ but the highest intensity of the peaks of AlN.

The excitation and emission spectra of these phosphors are plotted in Fig. 2. The excitation spectra show a broad band from the near-UV region to the visible light region. The band located at ca 240 nm is attributed to the electronic transition between the valence and the conduction band of the $CaAlSiN_3$ host. The peaks located at ca 320 and 460 nm are due to the 4f to 5d transition of Eu^{2+} ions. The broad emission band from 550 to 800 nm, recorded in all samples tested, is assigned to the allowed $4f^65d \rightarrow 4f^7$ transition of Eu^{2+} ions. The emission band of the phosphor produced with H_3BO_3 flux is blue shifted and its intensity is significantly lower compared to the emission of the other phosphors, specifically the flux-free phosphor and the phosphors with BaF_2, CaF_2, and NH_4F.

The increase in the intensity of the emission due to the addition of a flux can be attributed to the growth of the particle size, the narrowing of the particle-size distribution, and the increase of crystallinity: large grains decrease light scattering caused by the small particles; high crystallinity reduces the defects in the lattice and on the surface of the phosphor. Moreover, the blue shift of the emission peak should result from the weakening of the crystal field around Eu^{2+}. The distances between the atoms of Ca and Eu and the five nearest atoms of N in the $CaAlSiN_3$ without oxygen (2.4515 Å) are smaller than the distances in the same compound containing oxygen (2.4795 Å) [17]. Thus, the fact that H_3BO_3 is the only flux (among those tested in this study) that contains oxygen may be implicated in the crystalline regime (Fig. 1) and the photoluminescence spectra of the phosphors produced with H_3BO_3 (Fig. 2), as discussed previously.

Observation of the microstructure, presented in the SEM images in Fig. 3, supports the above discussion. The powder produced without fluxes (Fig. 3a) consists of small particles whose round edges suggest poor crystallization. The addition of the fluxes BaF_2 (Fig. 3b), CaF_2 (Fig. 3c), and NH_4F (Fig. 3d) apparently favors the production of uniform particles, generally bigger in size (compared to those shown in Fig. 3a) and with sharp edges (suggesting high crystallinity). All these features are much demanded to obtain excellent photoluminescence properties. In the powder produced with H_3BO_3 flux, big particles were also observed along with a large number of small particles. This finding provides fairly good support for the lowering of the intensity of the emission band in these phosphors (Fig. 2). Fig. 4 shows the particle size distribution of $CaAlSiN_3:Eu^{2+}$ with various kinds of flux. The particle size of the

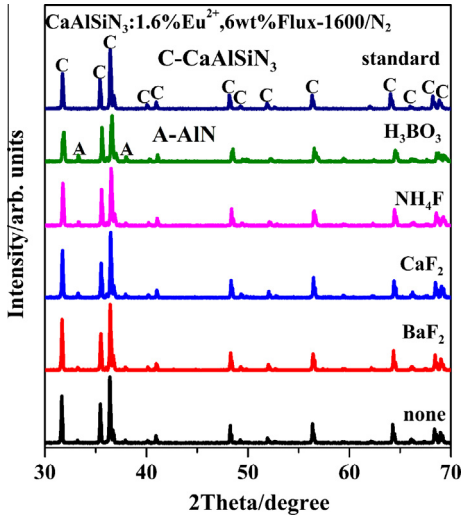

Fig. 1. X-ray diffractograms of $CaAlSiN_3:0.016Eu^{2+}$ phosphors, flux-free (none) and with addition of 6 wt% of different fluxes, BaF_2, CaF_2, NH_4F, and H_3BO_3, produced at 1600 °C for 4 h in N_2 flow.

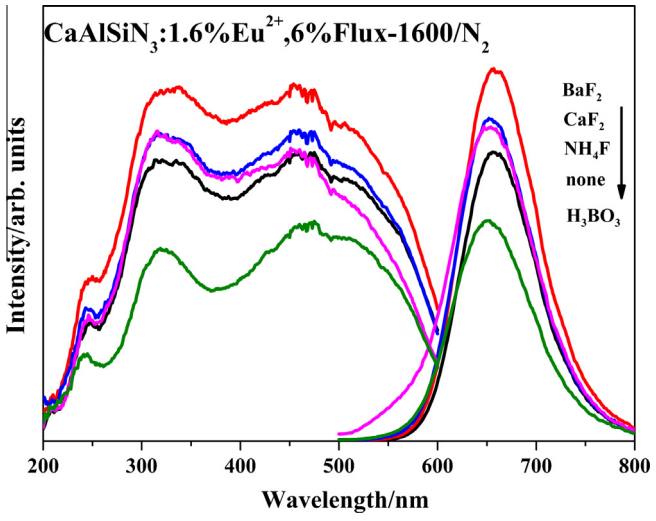

Fig. 2. Excitation and emission spectra of $CaAlSiN_3:0.016Eu^{2+}$ phosphors, flux-free (none) and with addition of 6 wt% of different fluxes, BaF_2, CaF_2, NH_4F, and H_3BO_3, produced at 1600 °C for 4 h in N_2 flow.

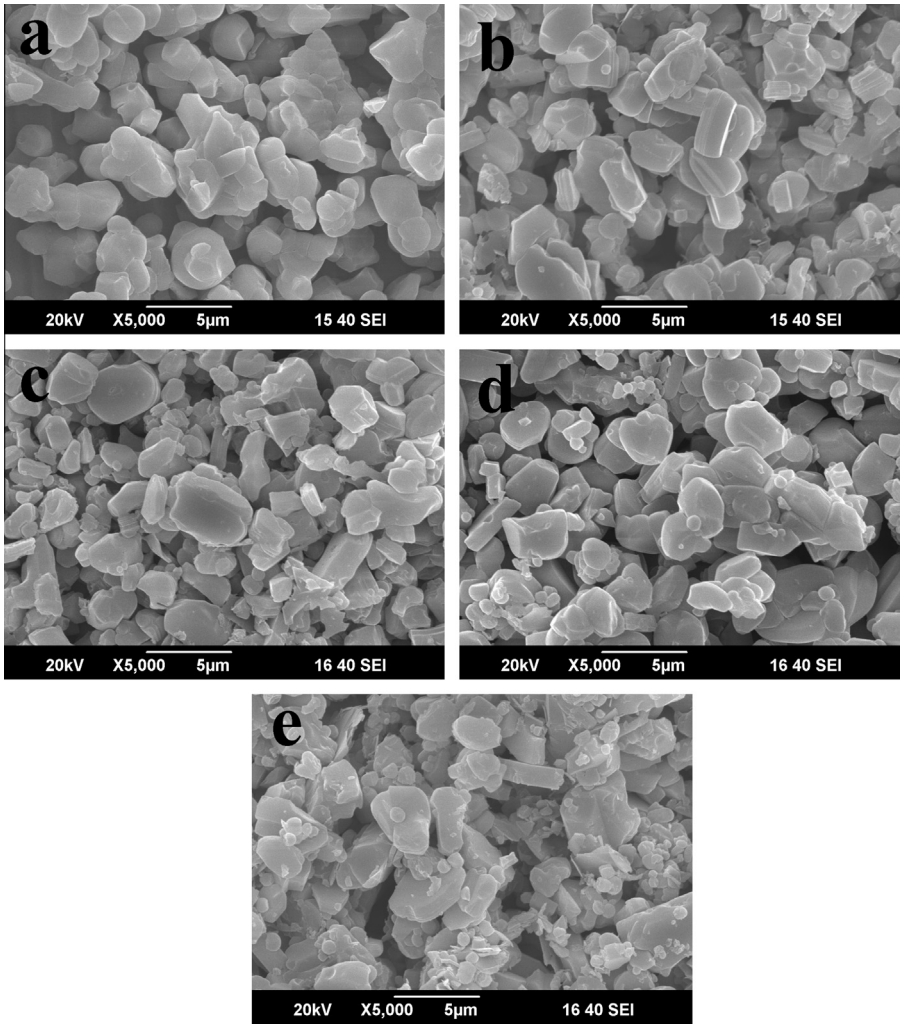

Fig. 3. Microstructure of $CaAlSiN_3$:0.016Eu^{2+} phosphors, (a) flux-free and with addition of 6 wt% of different fluxes, (b) BaF_2, (c) CaF_2, (d) NH_4F, and (e) H_3BO_3, produced at 1600 °C for 4 h in N_2 flow.

synthesized sample without any flux was 9.94 μm, whereas the particle sizes of the samples with BaF_2, CaF_2, NH_4F, and HBO_3 were 11.44, 11.20, 11.03, and 9.46 μm, respectively. This confirms that a good flux could promote grain growth and narrow grain size distribution.

The above experimental results show that the strongest emission band was obtained with the phosphors produced with BaF_2 flux. Thus, the following experiments focus on phosphors produced with BaF_2 flux.

First of all, the influence of firing temperature on the crystalline structure was investigated. Fig. 5 shows the diffractograms of $CaAlSiN_3$:0.016Eu^{2+} powders, flux-free (Fig. 5a) and with 6 wt% BaF_2 (Fig. 5b), produced at different temperatures between 1300 and 1800 °C. Comparison of the two diffractograms at 1300 °C (to better show the peaks, the intensities of the diffractograms at 1300 °C have been magnified by a factor of four) suggests that the addition of BaF_2 flux favors the increase of crystallinity (and consequently should reduce the formation temperature of $CaAlSiN_3$) and effectively suppresses the formation of other non-demanded secondary phases. Single-phase well-crystallized ceramic powder of $CaAlSiN_3$ was produced at 1400 and 1600 °C regardless of the addition of BaF_2. Firing at elevated temperatures (1700 and 1800 °C) caused a considerable reduction of crystallinity and formation of many impurity phases, likely due to decomposition of $CaAlSiN_3$ and volatilization of the raw materials.

The plots of the thermal analysis (DSC/TG curves) of the as-prepared materials (i.e. the powder mixtures of the raw materials) with and without BaF_2 are shown in Fig. 6. It is seen that the BaF_2-free powder loses about 20% of its weight between 1000 and 1400 °C (likely due to volatilization of Ca_3N_2), whereas there is a negligible weight loss in the powder-mixture with BaF_2. In the BaF_2-free batch, $CaAlSiN_3$ forms in a two-step mechanism, as indicated by the two endothermic peaks at 1105 and 1293 °C. It is suggested that Ca_3N_2(EuN) and Si_3N_4 forms at 1105 °C. The reaction of the more thermally stable AlN with Ca_3N_2(EuN) and Si_3N_4 occurs at 1293 °C to yield $CaAlSiN_3$. The X-ray diffractogram for 1300 °C in Fig. 5a seemingly supports this mechanism because the peaks due to AlN are clearly seen and the peaks of an unknown phase (designated by "U") were also registered; the latter can likely be attributed to the aforementioned intermediate phase formed above 1105 °C.

The presence of BaF_2 (Fig. 6) seemingly increases the reactivity of AlN (probably due to dissolution of AlN in BaF_2) since the broad endothermic peak at 974 °C suggests that the reaction to form $CaAlSiN_3$ occurs in one step and at a lower temperature. Moreover, the early formation of $CaAlSiN_3$ suppresses the volatilization of Ca_3N_2 (whose melting point is 1195 °C). The X-ray diffractogram for 1300 °C in Fig. 5b also supports this mechanism because the peaks due to AlN are weak and the peaks of the unknown phase (in Fig. 5a) were not registered at all.

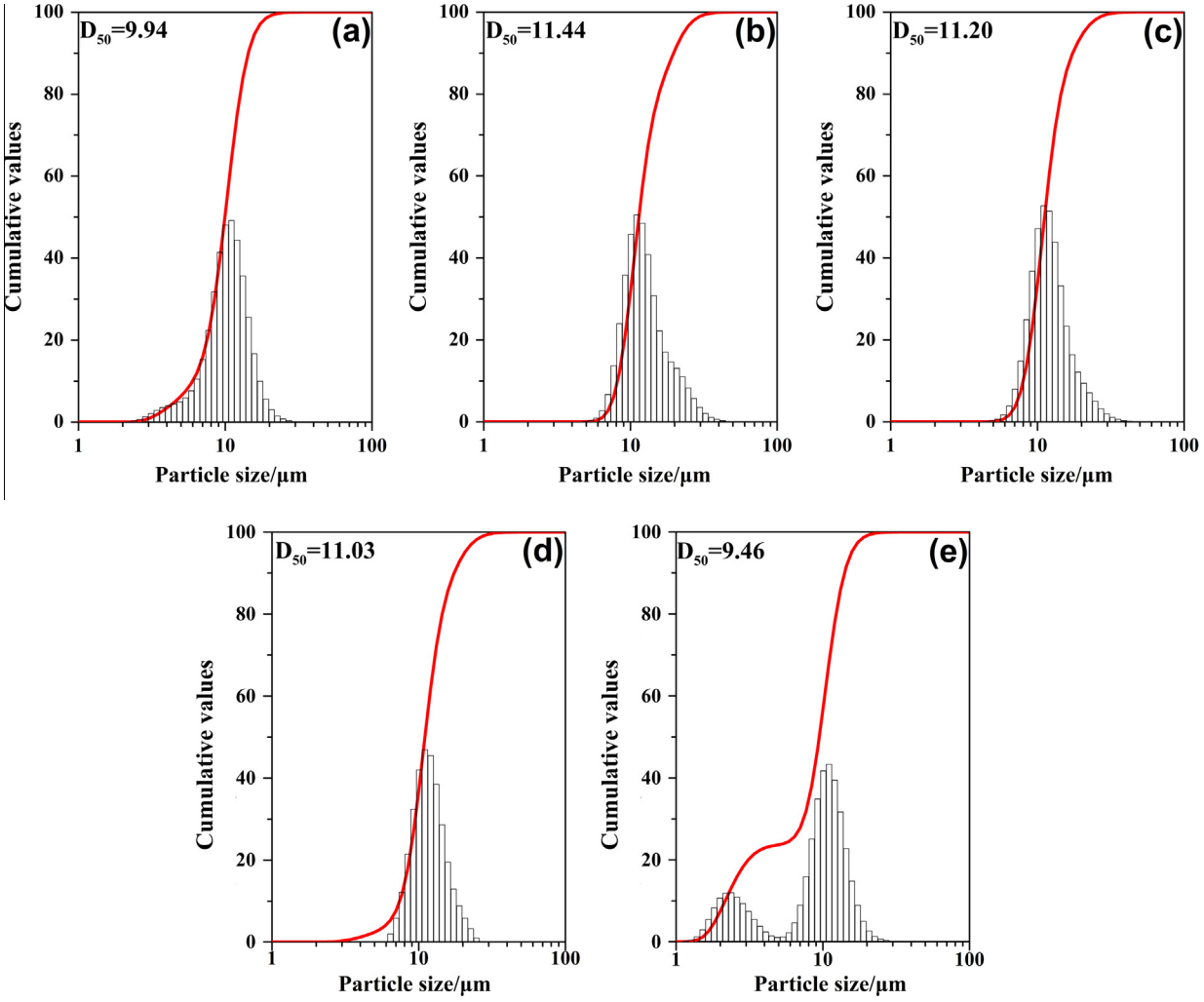

Fig. 4. Particle size distribution of $CaAlSiN_3:Eu^{2+}$ with various kinds of flux (a) none, (b) BaF_2, (c) CaF_2, (d) NH_4F, and (e) H_3BO_3.

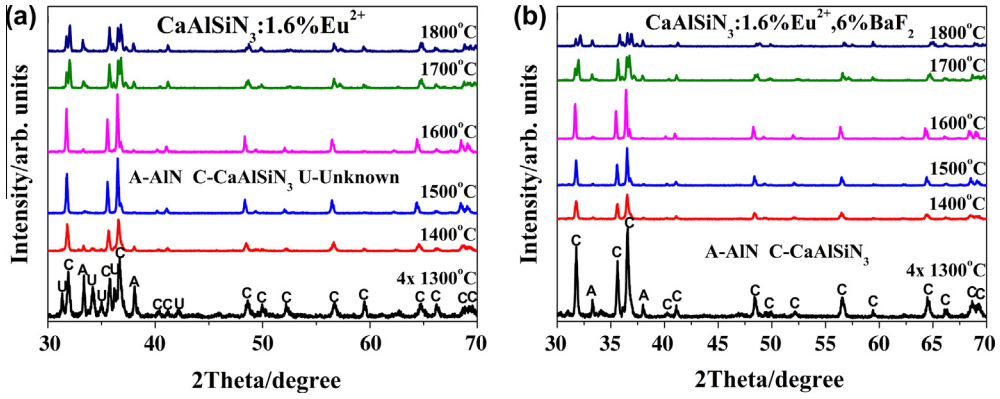

Fig. 5. X-ray diffractograms of $CaAlSiN_3:0.016Eu^{2+}$ phosphors, (a) flux-free and (b) with addition of 6 wt% of BaF_2, produced after firing for 4 h in N_2 flow at different temperatures. (To show better the peaks, the intensities of the diffractograms at 1300 °C have been magnified 4×.)

The influence of the N_2-pressure (static pressure of 0.5 MPa and N_2 flow) applied during the synthesis process on the maximum intensity of the emission band of $CaAlSiN_3:0.016Eu^{2+}$ phosphors produced at different temperatures with and without 6 wt% BaF_2 is shown in the plots in Fig. 7. In all cases, the addition of BaF_2 generally favors the increase in the intensity of emission. Moreover, the increase in firing temperature greatly increases the intensity of the emission up to a certain temperature, likely due to the increase of crystallinity. The reduction in intensity in the phosphors produced at very high temperatures is likely a result of decomposition and volatilization. The increase of the N_2-pressure up to 0.5 MPa causes a further increase in the intensity maxima which are reached at even higher temperatures (1700 °C), seemingly because the high nitrogen pressure suppresses volatilization.

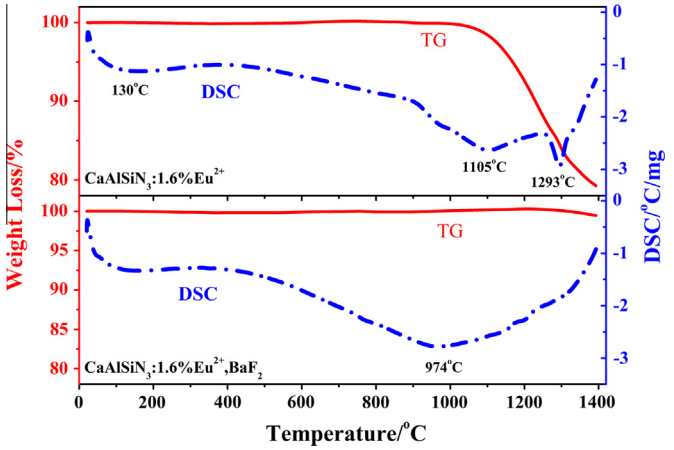

Fig. 6. Thermal analysis (DSC/TG curves) of the as-prepared materials with BaF_2 and without BaF_2.

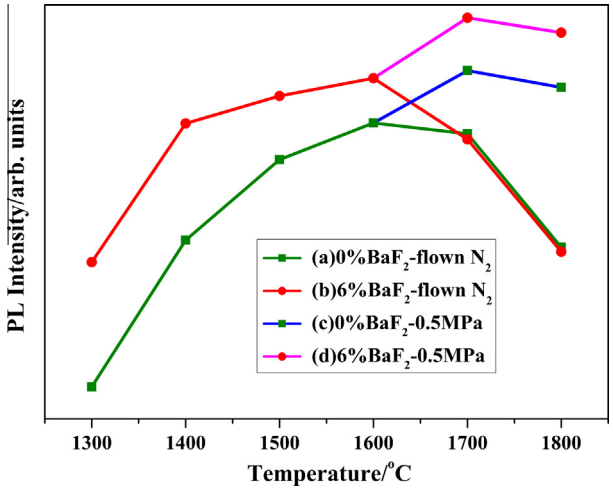

Fig. 7. Maxima of the intensities of emission of the $CaAlSiN_3$:0.016Eu^{2+} phosphors: (a) and (c) BaF_2-free, (b) and (d) with 6 wt% BaF_2; fired at different temperatures and gas-pressures: (a) and (b) N_2 flow (designated as "1 atm"), (c) and (d) static N_2 0.5 MPa.

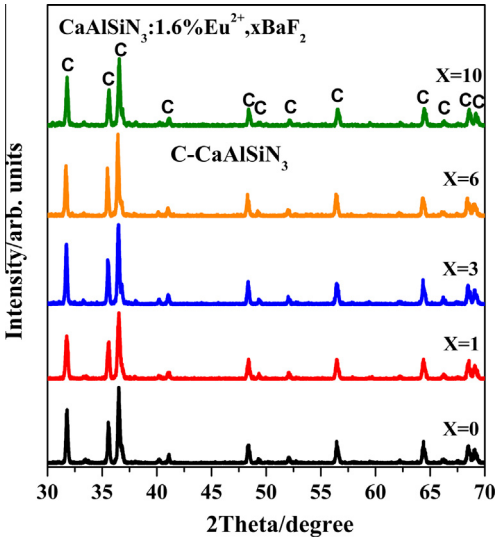

Fig. 8. X-ray diffractograms of $CaAlSiN_3$:0.016Eu^{2+} phosphors, flux-free and with different amounts of BaF_2, produced at 1600 °C for 4 h in N_2 flow.

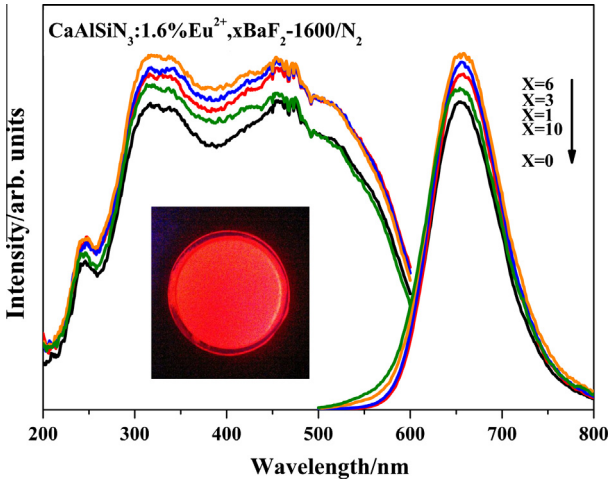

Fig. 9. Excitation and emission spectra of $CaAlSiN_3$:0.016Eu^{2+} phosphors, flux-free and with different amounts of BaF_2, produced at 1600 °C for 4 h in N_2 flow. The inset shows the luminescence photograph of the $CaAlSiN_3$:0.016Eu^{2+} phosphor with 6 wt% BaF_2 excited at 360 nm in a UV box.

It is also worth noting that the beneficial effect of BaF_2 on enhancing the intensity of emission intensity is not annulled even at those very high temperatures. It can also be noticed that the BaF_2-free phosphor produced at 1700 °C with 0.5 MPa N_2 has the same intensity of emission as the $CaAlSiN_3$:Eu^{2+} phosphor with BaF_2 calcined at 1600 °C under N_2 flow.

Consequently, both the addition of BaF_2 and increasing nitrogen pressure favor the increase in the intensity of emission of the $CaAlSiN_3$:Eu^{2+} phosphor, but BaF_2 is certainly more cost-effective. Thus, the influence of the amount of BaF_2 on the crystalline regime (Fig. 8) and the photoluminescence properties (Fig. 9) of the produced $CaAlSiN_3$:Eu^{2+} phosphors was investigated. With regard to the former property (Fig. 8), it seems that there is no perceptible influence of the amount of BaF_2 on the crystalline structure of the produced phosphors since they were all well-crystallized single-phase ceramic powders of $CaAlSiN_3$. However, the amount of BaF_2 has a strong influence on the intensity of the emission. In particular, the increase in the amount of BaF_2 favors an increase in the intensity, and a maximum was achieved in the phosphor with 6 wt% BaF_2. The intensity decreased with 10 wt% BaF_2. The inset of Fig. 9 shows the luminescence photograph of the $CaAlSiN_3$:0.016Eu^{2+} phosphor with 6 wt% BaF_2 excited at 360 nm in a UV box, and the CIE color coordinate calculated from the recorded spectra (x = 0.654, y = 0.345) indicates its high color saturation.

4. Conclusions

This work has shown that the incorporation of the proper amount of BaF_2 flux in the synthesis of $CaAlSiN_3$:Eu^{2+} phosphor via solid state reaction carried out at optimum conditions of temperature and N_2 atmosphere can maximize the intensity of emission because it can greatly improve the morphology and crystallinity of the particles of the produced powders. The experimental results showed that the presence of BaF_2 reduces the temperature of formation of $CaAlSiN_3$:Eu^{2+} because it enhances the reactivity of AlN at lower temperatures and modifies the mechanism of formation of $CaAlSiN_3$ from a two-step to a one-step reaction. The aforementioned beneficial role of BaF_2 is not jeopardized at temperatures as high as 1700 °C. These results qualify the production of high performance $CaAlSiN_3$:Eu^{2+} phosphors via the solid state reaction synthesis method with the aid of BaF_2 flux for further consideration and experimentation in white-LED technology.

Acknowledgements

This research was supported by the National Science Foundation of China (Nos. 51072191 and 11179037), National Basic Research Program of China (973 Program, 2012CB922004), USTC-NSRL association funding (KY2060140005) and Anhui Provincial Education Department (KJ2012A289).

References

[1] R.-J. Xie, N. Hirosaki, M. Mitomo, K. Sakuma, N. Kimura, Appl. Phys. Lett. 89 (2006) 241103.
[2] G.-Y. Lee, J.Y. Han, W.B. Im, S.H. Cheong, D.Y. Jeon, Inorg. Chem. 51 (2012) 10688–10694.
[3] T. Wang, J. Yang, Y. Mo, L. Bian, Z. Song, Q.L. Liu, J. Lumin. 137 (2013) 173–179.
[4] L. Yu, Y. Hua, H. Chen, D. Deng, H. Wang, H. Ma, S. Xu, Opt. Commun. 315 (2014) 83–86.
[5] J.-Y. Tang, Y.-M. He, L.-Y. Hao, X. Xu, S. Agathopoulos, J. Mater. Res. 28 (2013) 2598–2604.
[6] X. Song, H. He, R. Fu, D. Wang, X. Zhao, Z. Pan, J. Phys. D: Appl. Phys. 42 (2009) 065409.
[7] X. Song, R. Fu, S. Agathopoulos, H. He, X. Zhao, X. Yu, J. Am. Ceram. Soc. 94 (2011) 501–507.
[8] J.-Y. Tang, X.-F. Yang, C. Zhan, L.-Y. Hao, X. Xu, W.-H. Zhang, J. Mater. Chem. 22 (2012) 488–494.
[9] J. Liu, X. Wang, T. Xuan, H. Li, Z. Sun, J. Alloys Comp. 593 (2014) 128–131.
[10] X. Xu, J.Y. Tang, T. Nishimura, L.Y. Hao, Acta Mater. 59 (2011) 1570–1576.
[11] Z. Yang, Y. Wang, Z. Zhao, J. Alloys Comp. 541 (2012) 70–74.
[12] T. Suehiro, N. Hirosaki, R.-J. Xie, T. Sato, Appl. Phys. Lett. 95 (2009) 051903.
[13] Y. Zhou, Y.-I. Yoshizawa, K. Hirao, Z. Lences, P. Sajgalik, J. Eur. Ceram. Soc. 31 (2011) 151–157.
[14] Y.Q. Li, J.E.J. van Steen, J.W.H. van Krevel, G. Botty, A.C.A. Delsing, F.J. DiSalvo, G. de With, H.T. Hintzen, J. Alloys Comp. 417 (2006) 273–279.
[15] V.D. Luong, W. Zhang, H.-R. Lee, J. Alloys Comp. 509 (2011) 7525–7528.
[16] L. Wang, H. Ni, Q. Zhang, F. Xiao, Mater. Lett. 112 (2013) 84–86.
[17] X. Piao, K.-I. Machida, T. Horikawa, H. Hanzawa, Y. Shimomura, N. Kijima, Chem. Mater. 19 (2007) 4592–4599.
[18] H. Watanabe, N. Kijima, J. Alloys Comp. 475 (2009) 434–439.
[19] S. Lee, K.-S. Sohn, Opt. Lett. 35 (2010) 1004–1006.
[20] J. Yang, T. Wang, D. Chen, G. Chen, Q. Liu, Mater. Sci. Eng., B 177 (2012) 1596–1604.
[21] M. Kubus, H.J. Meyer, Z. Anorg, Z. Anorg. Allg. Chem. 639 (2013) 669–671.
[22] M. Mikami, K. Uheda, N. Kijima, Phys. Status Solidi A 203 (2006) 2705–2711.
[23] T. Suehiro, R.-J. Xie, N. Hirosaki, Ind. Eng. Chem. Res. (2014). 140206141348006.
[24] H.S. Kim, K.-I. Machida, T. Horikawa, H. Hanzawa, Chem. Lett. 43 (2014) 533–534.
[25] Y.Q. Li, N. Hirosaki, R.J. Xie, T. Takeda, M. Mitomo, Chem. Mater. 20 (2008) 6704–6714.
[26] K. Uheda, N. Hirosaki, Y. Yamamoto, A. Naito, T. Nakajima, H. Yamamoto, Electrochem. Solid-State Lett. 9 (2006) H22–H25.
[27] L.-J. Yin, W. Yu, X. Xu, L.-Y. Hao, A. Simeon, J. Am. Ceram. Soc. 94 (2011) 3842–3846.
[28] L. Liu, R.-J. Xie, C. Zhang, N. Hirosaki, Materials 6 (2013) 2862–2872.